Lowland Technology International 2019; Volume 21 (Issue 2.): 80-89
International Association of Lowland Technology (IALT): ISSN 1344-9656

Research Paper

Correlation Between Shear Wave Velocity and Liquefaction Resistance for Sandy Soils With A Shearing History Using Cyclic Tri-axial Tests

G. J. Liu[1], N. Yasufuku[2] and R. Ishikura [3]

ARTICLE INFORMATION

Article history:

Received: 03 January, 2019
Received in revised form: 18 March, 2019
Accepted: 03 May, 2019
Publish on: 5 September, 2019

Keywords:

Sand,
cyclic test,
bender elements,
shear wave velocity,
shear history,
liquefaction resistance

ABSTRACT

Many serious disasters induced by ground liquefaction were reported in earthquakes with multiple shocks recently. The level of damage was considered because the liquefaction resistance changed with the pre-shearing from these shocks. Velocity of shear wave with small strain was used as an index for assessing liquefaction resistance because it is also influenced by similar factors as liquefaction resistance in soils. The effects of shearing history on the liquefaction resistance was discussed in this study. Cyclic tri-axial apparatus with bender elements was assembled to conduct the laboratory tests. Saturated sand was prepared as the test material. Both shear wave velocity and changes of liquefaction resistance were investigated during test process. The results indicated that shear wave velocity can be used to evaluate the liquefaction resistance and assess the effects from pre-shearing in sand. However, the correlation was influenced by initial relative density and stress state.

1. Introduction

1.1 The 2016 Kumamoto earthquake

Soil liquefaction induced damage plays an important role in geo-disasters considering the unique geological conditions of Japan. Many earthquakes induced geo-disasters were reported in recent years in extreme events such as the 2011 Great East Japan Earthquake and the 2016 Kumamoto Earthquakes. Fig. 1 shows the time history of earthquake acceleration in two great shocks of the 2016 Kumamoto Earthquakes as reported by the Japan Meteorological Agency (JMA, 2016). The data at Mashiki town which were collected at the location very close to the epicenters showed that the two great shocks struck there within a very short time. The foreshock (M6.2) struck there on April 14, and about 28 hours later, the main shock (M7.0) hit the same region again in the middle of the night on April 15.

1.2 Liquefaction resistance affected by shearing history in soils

According to the field investigation reported by Mukunoki et al. (2016), the two major shocks were the main reason for the extreme damage induced by soil liquefaction. Many sites were not affected by liquefaction or damaged very slightly during the foreshock. However, these sites were destroyed or badly damaged by soil liquefaction in the main shock, which was of a magnitude

[1] Corresponding author, Ph.D. candidate, Department of Civil and Structural Engineering, Kyushu University, Fukuoka 819-0395, JAPAN, liuguojunjj0@163.com
[2] Professor, Department of Civil and Structural Engineering, Kyushu University, Fukuoka 819-0395, JAPAN, yasufuku@civil.kyushu-u.ac.jp
[3] Associate Professor, Department of Civil and Structural Engineering, Kyushu University, Fukuoka 819-0395, JAPAN, ishikura@civil.kyushu-u.ac.jp
Note: Discussion on this paper is open until March 2020

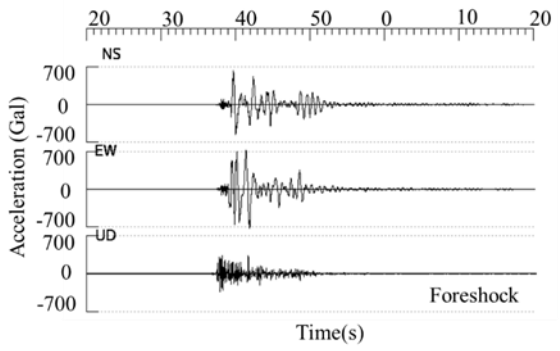

(a). Foreshock on April 14, 2016

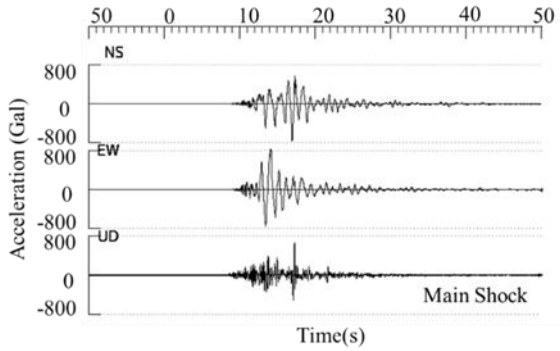

(b). Main shock on April 16, 2016

Fig. 1. (a) and (b). Time history of acceleration observed at Mashiki Town by JMA (2016).

beyond prediction. This kind of damage occurred not only at Mashiki town and its vicinity, but also at almost all of Kumamoto plain and Aso basin. The foundations of many buildings, embankments, farmlands were damaged and even some landslides on hills with a gentle gradient were observed that were directly or potentially caused by soil liquefaction.

A series of laboratory tests conducted by Tatsuoka and Ishihara (1974), Ishihara et al. (1975, 1978) and Yamada (2010) found that liquefaction resistance of sandy soils, affected by shearing history dropped greatly. Relative density probably increased after this process and this was commonly considered as beneficial for preventing liquefaction. Therefore, according to their results, the changes of anisotropy caused by the pre-shearing exceeding the yield limitation were the main factor to cause the great reduction of liquefaction resistance. However, the changes of anisotropy could not be observed directly in in-situ investigation. Thus, it was considered both important and urgent to find a reliable and quick non-destructive method to evaluate the changes of liquefaction resistance affected by shear history. Velocity of shear wave with small strain was proposed for assessing the liquefaction potential because it was regarded as an index determined by particle conditions, stress states, stress history, and geologic age (Dobry et al. 1981, Andrus and Stokoe 2000).

1.3 Correlation between shear wave velocity and liquefaction resistance-

The correlations between shear wave velocity and liquefaction resistance was developed by Andrus and Stokoe (2000) using the field data in historical earthquakes from 1906 to 1995 (Fig. 2). Particle conditions, stress state and geological age were taken into consideration. The lower bounds of liquefiable soils with different fines contents were proposed. Liquefaction resistance in the boundaries increases with increasing stress-corrected shear wave velocity V_{s1}. In addition, the greater resistance appeared in soils with the greater fines content at a given V_{s1} in most of range. However, for these liquefied sites, the effects of one shock or multiple shocks during the earthquakes were not distinguished. In other words, the factor of shear history which was produced in a relative short interval during the earthquakes, compared with geological age was not considered. Therefore, the effect of shear history on the correlation between shear wave velocity and liquefaction resistance was investigated by cyclic tri-axial tests in this study.

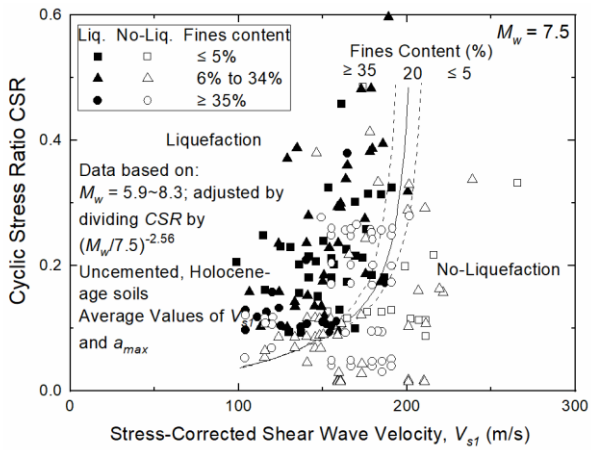

Fig. 2. Liquefaction boundary curve estimated by stress-corrected shear wave velocity based on field investigation (Andrus and Stokoe 2000).

2. Cyclic tri-axial testing with bender elements

Cyclic tri-axial compression apparatus was assembled with bender elements for the laboratory tests in the study. This apparatus could clearly exhibit variation of both stress-strain and shear wave velocity during the entire test process. Besides, the parameters such as stress state, saturation degree and extent of shearing history could also be controlled accurately. Therefore, it

provided the possibility to assess the correlation between liquefaction resistance and shear wave velocity especially for the soils with a given shear history.

2.1 Specimen's preparation and test process

Samples of Toyoura sand with different relative densities (D_r = 60%~80%) were used as the test materials in the experiments. The physical properties are showed in Fig. 3 and Table 1. The specimens were prepared by water pluviation in tri-axial apparatus with size: 100 mm in height and 50 mm in diameter. In order to ensure that the sand was completely saturated (B-Value ≥ 0.95) in the tests, CO_2 was used to eject the residual air in the sand. Deaired water was then injected slowly from the lower porous stone to fill the voids in sand. After that, the specimens were consolidated normally at confining pressure σ'_{c0} = 100 kPa under drained condition. Enough time was allowed for consolidation under this confining pressure. After the normal consolidation, the specimens were tested by cyclic load under undrained condition until liquefaction appeared. The liquefied sand was consolidated again under the same conditions as in the first normal consolidation. Then the re-consolidated sand was tested until it liquefied again.

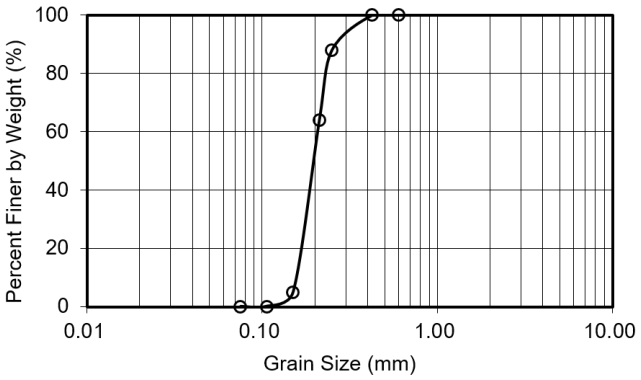

Fig. 3. Cumulative grain size distribution of Toyoura sand

Table 1. Physical properties of Toyoura sand

Table 1. Physical properties of Toyoura sand

Specific gravity G_s	2.643
Maximum void ratio e_{max}	0.977
Minimum void ratio e_{min}	0.606

The cyclic load followed the sinusoidal wave with a frequency of 0.1 Hz. The cyclic stress ratio $\sigma_d/2\sigma'_0$ (CSR) varied from 0.2 to 0.4 which was set with the same level both in the first and second tests. Shear strain with double amplitudes (DA.) up to 5% was commonly adopted as the criterion for adjudging soil liquefaction in cyclic tri-axial tests.

The typical cyclic load and the results are shown in Fig. 4 Fig. 5, for sand with initial D_r = 60%. It was found that both excess pore water pressure and shear strain in the second test increased faster than in the first test. Moreover, the rate of change of shear strain in the first test increased progressively, unlike, for the second test which changed greatly in the first 1~2 cycles. Similar results were also obtained in other samples with different relative densities and CSR.

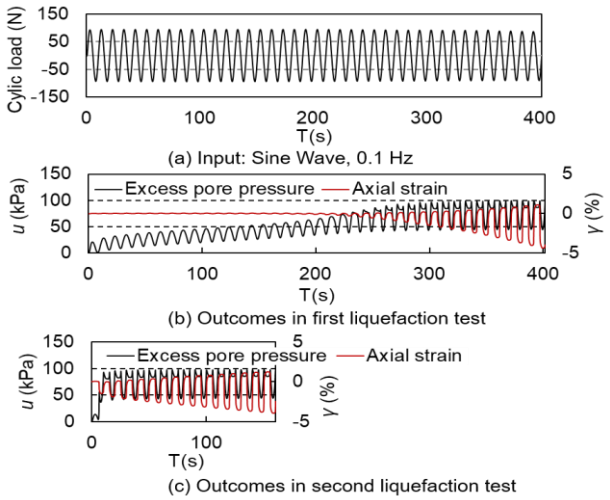

Fig. 4. Typical test results in first and second liquefaction tests (Initial D_r = 60%).

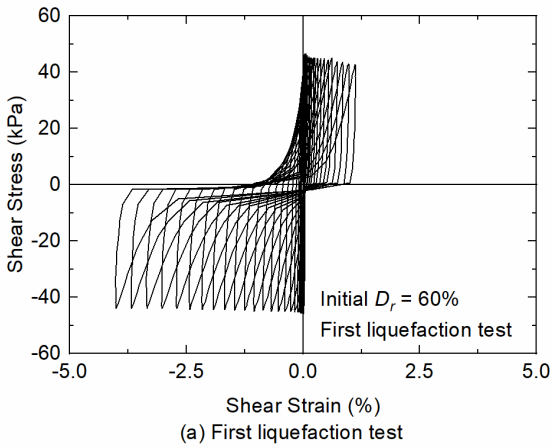

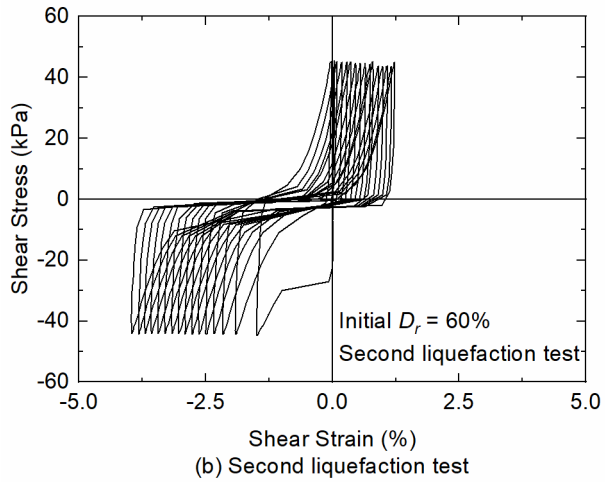

Fig. 5. Figure (a), and (b) Typical shear stress-strain in first and second liquefaction tests.

2.2 Measurement method of shear wave velocity

A couple of bender elements and a measurement system for shear wave were assembled on the cyclic tri-axial compression apparatus, as shown in Fig. 6. A single sinusoidal shear wave was generated from the upper side of the bender element and passed through the soil specimen, before being received by the lower bender element and recorded by the oscilloscope. At the same time, the other signal of shear wave was sent directly from the generator and it was also received and recorded by the oscilloscope. Thus, the travel time of the two signals is different. The travel time of the shear wave inside the specimen is denoted as ΔT. Fig. 7. shows a typical wave that was recorded. Several methods for the determination of shear wave velocity have been proposed previously such as first and second wave arrival with characteristic points suggested by Arulnathan et al. (1998) and Lee and Santamarina (2005).

In this study, the velocity of shear wave could be obtained by peak-to-peak of first wave arrival using the simplified expression according to Japanese Geotechnical Society (JGS) criterion (2004) as shown in Eq. [1]:

Shear wave velocity: $$V_s = \frac{L}{\Delta T} \quad [1]$$

Where, L = Length between Top-to-Top of bender elements.

Shear wave velocities were measured for the normally consolidated specimens, and for each load cycle during the cyclic tests process until the soils were liquefied (DA. = 5%). Thus, the variation trend of shear wave velocity during cyclic tests could be obtained. The measurement procedures for the re-consolidated process and second cyclic tests were then repeated.

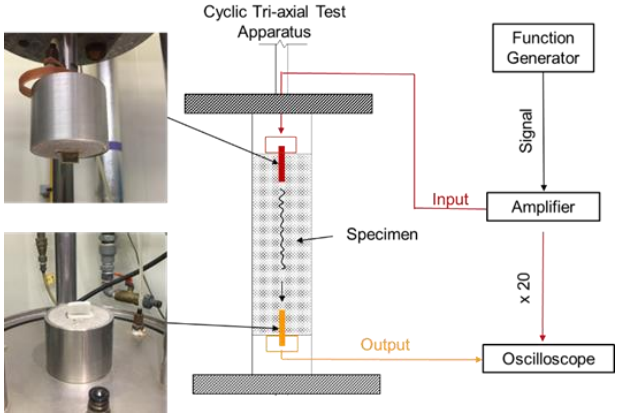

Fig. 6. Illustration of cyclic tri-axial test apparatus with bender elements

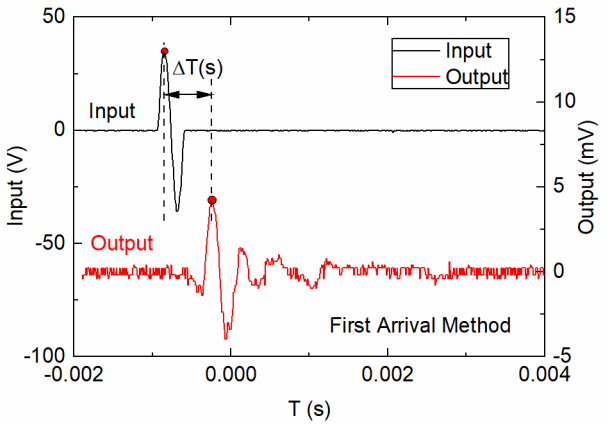

Fig. 7. Measurement of ΔT from the results of bender elements

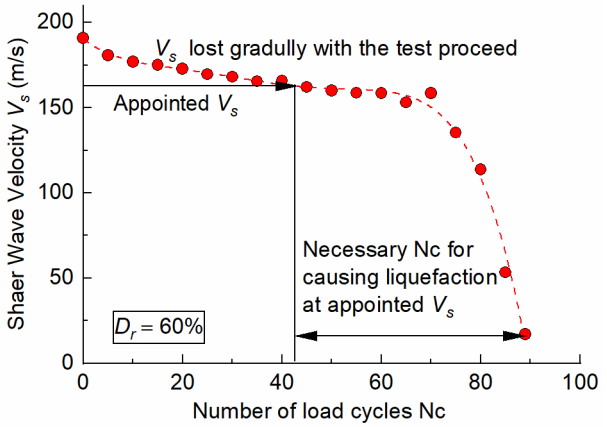

Fig. 8. Typical test results of V_s varied during test process carried from sand with D_r = 60%.

The typical variation of shear wave velocity measured during the entire cyclic tests progress for the sand with D_r = 60% is shown in Fig. 8. The variation tendency was very similar for different test conditions, and could be summarized as: 1) the maximum velocity appeared in initial state just after the consolidation (or re-consolidation); 2) velocity decreased gradually by shearing; 3) the sharp droopiness started with the interval from 150 m/s to 100 m/s, and, the velocity decreased at a faster rate while it reduced to less than 100 m/s (within only few cycles before liquefaction). Therefore, the range of shear velocity from 100 m/s to 200 m/s is of primary concern.

3. Effects of shear history with undraining process on the correlation between shear wave velocity and liquefaction resistance

Shear wave velocity in soils gradually decreased from the pre-shearing as shown in Fig. 8. Therefore, shear wave velocity could be regarded as the index to present the extent of pre-shearing for soils, meanwhile, the residual resistance of liquefaction also could be assessed by the number of residual load cycles. Therefore, the correlation between current shear wave velocity and residual liquefaction resistance could be developed based on the given shear history. In order to assess the influence from pre-shearing, the given velocity was adopted as the index to represent the extent of shear history in this study. It is worth mentioning that previous studies (Tokimatsu et al. 1986) used the given shear strain as index. The cyclic load before the given V_s was considered as the pre-shearing load while that after the given V_s was considered as the applied cyclic load for causing liquefaction

3.1 Effect of shear history on the correlation under same relative density

The extent of pre-shearing was controlled as the unique variable in sand with the same relative density. Firstly, several specimens of sand with D_r = 60% were prepared with the same conditions and were then tested by different cyclic shear stress. Results from Fig. 8 were used to determine the correlation between shear wave velocity and residual liquefaction resistance and Fig. 9 was thus plotted. All cyclic tests were conducted under undraining condition; thus, the relative density was considered constant during cyclic test process. The initial state of shear wave velocity at around 200 m/s displayed the greatest liquefaction resistance. The liquefaction resistance dropped with the shear wave velocity decreasing from 200 m/s to 120 m/s. Fig. 10 shows similar results in the sand prepared with a denser relative density of around 70%.

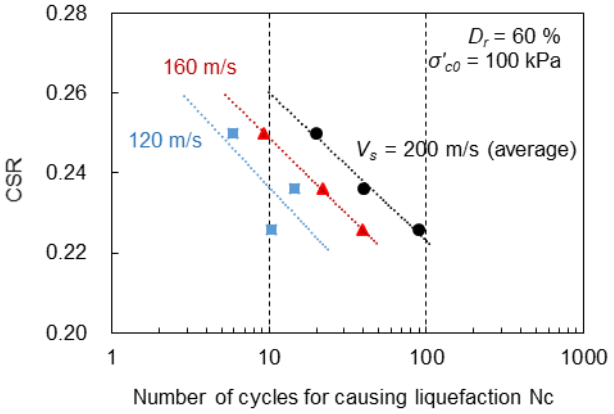

Fig. 9. Liquefaction resistance of medium sand affected by pre-shearing

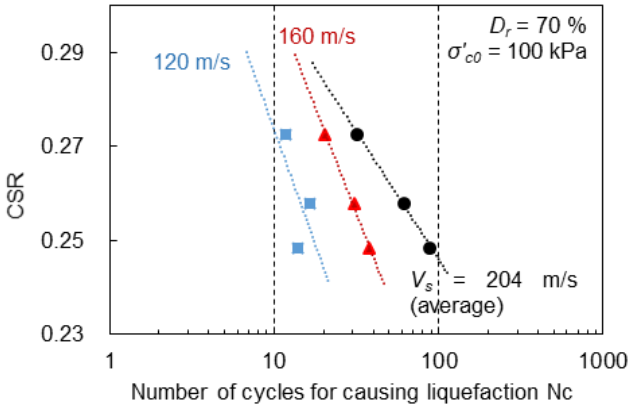

Fig. 10. Liquefaction resistance of medium-dense sand affected by pre-shearing

3.2 Effect of shear history on the correlation between different relative densities

All test cases were prepared under the same condition by a normal consolidation. The applied shear stress was thus considered as independent of liquefaction resistance and the relative density was the only variable factor at a given shear wave velocity. Fig. 11 shows the comparison of liquefaction resistance between the sands with different relative densities at given shear wave velocities. Initially, the shear wave velocities were very close at around 200 m/s though there was a great difference in liquefaction resistance.

This probably indicated that the effective confining pressure affects the shear wave velocity primarily, while,

the relative density affects liquefaction resistance significantly. The great difference also appeared when a given pre-shearing of shear wave velocity at 160 m/s and 120 m/s was applied to the sands. However, it potentially depended on the shear stress. The turning point was probably located at CSR = 0.21 for 160 m/s and 120 m/s respectively between the two relative densities. Therefore, if the applied CSR is greater than the turning point, denser sand achieved the greater liquefaction resistance; otherwise, looser sand achieved the greater resistance. For the initial states, the potential turning point could be considered as existing very far away.

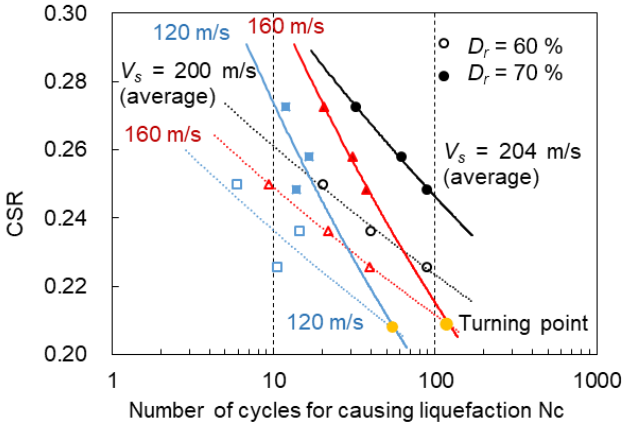

Fig. 11. Comparison of the liquefaction resistance affected by pre-shearing with deferent relative densities

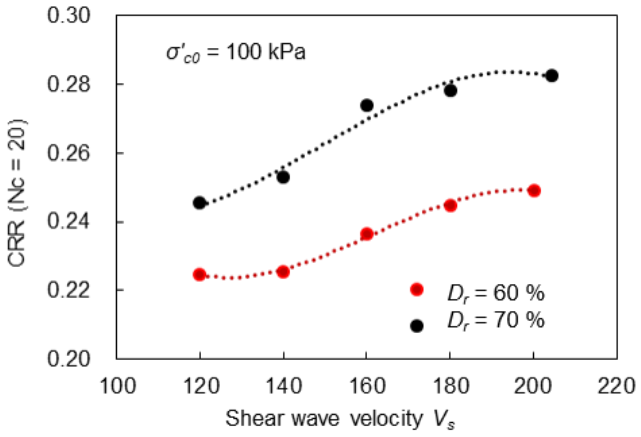

Fig. 12. Effect of relative density on the relationship between liquefaction resistance and shear wave velocity

Based on Fig. 11, the liquefaction resistance could be obtained by the given number of cycles and the given shear wave velocities. The CSR at Nc = 20 was commonly used as the liquefaction resistance. The comparison of liquefaction resistance between the two relative densities is shown in Fig. 12. The result indicated the greater liquefaction resistance always occurred in the sand with the higher relative density at the same shear wave velocity. Consequently, the effect of relative density is nonnegligible on the correlation to assess liquefaction resistance.

4. Effects of liquefied-reconsolidated process on the correlation between shear wave velocity and liquefaction resistance

This section extended the pre-shearing to an extreme condition to induce liquefaction once in sand. The liquefied sand was then again re-consolidated at the same confining pressure of 100 kPa under drainage condition. This process was named as “Liquefied-Reconsolidated process” in this study. The influence from B-value, relative density was discussed. Finally, a comparison of the correlation was conducted between laboratory-based data and field-based data.

4.1 Relationship between B-value and shear wave velocity

Shear wave velocity was measured just after first consolidation and liquefied-reconsolidated process. The velocities in Fig. 13 were arranged corresponding relating to the B-value of sand. Saturation degree in all samples could be considered being very closed to 100% (Lade and Hernandez 1977). Shear wave velocity in oven-dried sand was measured at around 240 m/s. Thus, it could be predicted that shear wave velocity decreases gradually with increasing of saturation degree. However, when B-value ≥ 0.8 (*Sr.* ≥ 99.50%), the shear wave velocity increased with increasing greater of B-value in sand both after normal consolidation and liquefied-reconsolidated process. Furthermore, the performance of shear wave velocity was influenced by liquefied-reconsolidated process and the value decreased some degrees after sand was pre-sheared during this process. The difference became larger in the sand with relative lower B-value.

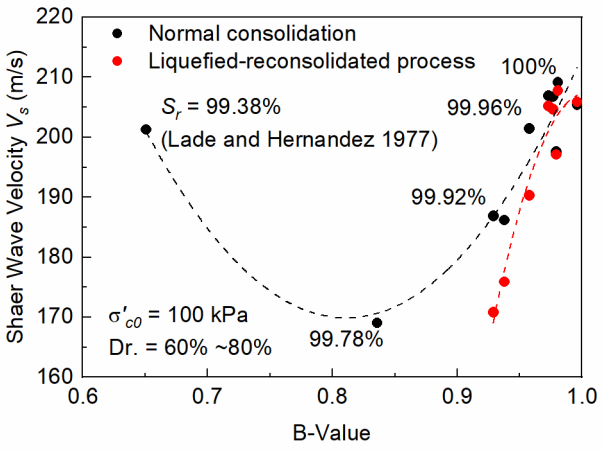

Fig. 13. Comparison of V_s after consolidation and re-consolidation with B-Value.

4.2 *Changes of shear wave velocity and relative density by liquefied-reconsolidation process*

Relative density played an important role on the correlation for pre-sheared sand with an undraining process. Thus, it was also worth discussing its effect on sand that had suffered liquefied-reconsolidated process. The relative densities and their corresponding shear wave velocities after normal consolidation and liquefied-reconsolidated process was plotted in Fig. 14.

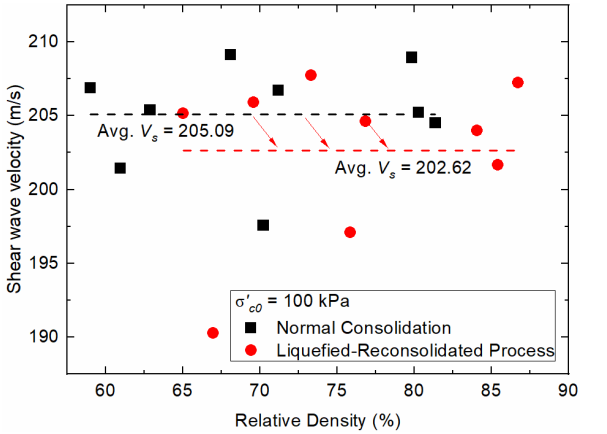

Fig. 14. Effect of relative density on V_s after two consolidation processes

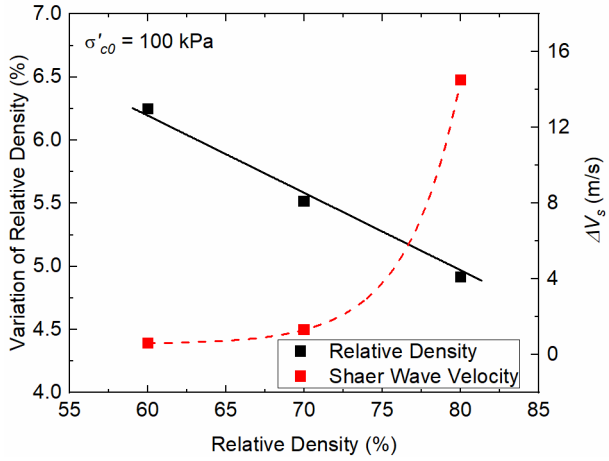

Fig. 15. Comparison of the variation of relative density and V_s between consolidation and re-consolidation processes

Table 2. Number of cycles representative of different magnitude earthquakes

Magnitude	Number of representative cycles at 0.65 τ_{max}
8.5	26
7.5	15
6.75	10
6	5-6
5.25	2-3

The results do not show a clear correlation between relative densities and shear wave velocities after each self-process. For velocities were from 197.5 m/s to 205 m/s for sand after normal consolidation and were from 190 m/s to 207.5 m/s for sand that had suffered liquefied-reconsolidated process irrespective of the relative densities. The averaged shear wave velocity decreased slightly from 205.09 m/s to 202.62 m/s. The distribution of relative density moved some distance to increasing direction integrally in all cases. The changes of relative density and shear wave velocity between the two processes between the averaged values at D_r = 60%, 70%, 80% are shown in Fig. 15.

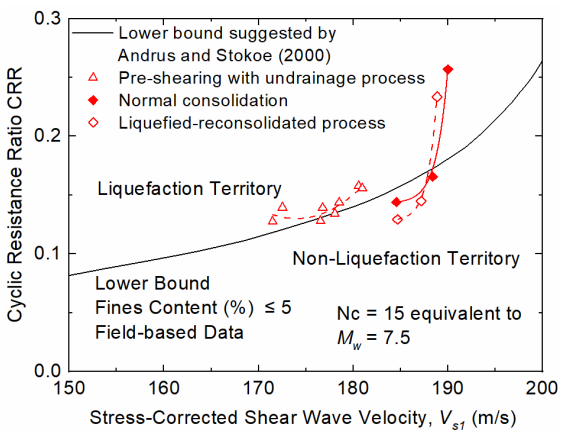

Fig. 16. Comparison between laboratory-based data of pre sheared sand and lower-bound curve based on field data

The results disclosed that: 1） relative density increased about 5.0% ~6.5% while shear wave velocity decreased about 0 ~16 m/s; 2) the difference of relative density became smaller with increasing relative density of sand. The proportionality could be considered as a constant; 3) On the contrary, the changes of shear wave velocity became larger with increasing relative density. Furthermore, the rate of the change was faster for the sand with greater relative density.

4.3 *Comparison between laboratory-based data and field-based data for pre-sheared sandy soils*

In order to compare data from laboratory and field, both shear wave velocity and liquefaction resistance needed to be converted to the field conditions by the following expressions:

4.3.1 *Stress-corrected shear-wave velocity*

For shear wave velocity to be considered as the index, much depends on the state of stress in the soil (Hardin and Drnevich, 1972). It could be corrected with the reference overburden stress in a similar way as the traditional procedure for correcting SPT blow count and CPT trip resistance by (Robertson et al., 1992; Andrus and Stokoe, 2000):

$$V_{s1} = V_s C_v = V_s \left(\frac{P_a}{\sigma'_v} \right)^{0.25} \quad [2]$$

Where, V_{s1} = Overburden stress-corrected shear wave velocity; V_s = measured shear wave velocity in situ; C_v = conversion factor to correct V_s for overburden pressure; P_a = reference stress of 100 kPa; σ'_v = effective overburden stress. In field investigation, σ'_v determined majorly by depth and ground water level, is corresponded to the σ'_h with K_0 = lateral earth pressure coefficient at rest.

$$\sigma'_h = K_0 \sigma'_v \quad [3]$$

Where, σ'_h = horizontal effective stress; the velocity at which shear wave propagates along the soil in current condition can be determined by the empirical formula (Roesler, 1979; Bellotti et al. 1996).

$$V_s = C_s \sqrt{F(e) \sigma'^{na}_a \sigma'^{nb}_b \sigma'^{nc}_c} \quad [4]$$

Where, $F(e)$ = void ratio function; σ'_a = principal effective stress along the propagation direction; σ'_b = principal effective stress in the direction of particle motion; σ'_c = the effective principal stress which acts on the plane defined by the propagation direction of shear wave and particle motion; and C_s = constant determined empirically. Since the cyclic tri-axial tests in this study were conducted under isotropic condition, $nc \approx 0$; and $na \approx nb \approx n$ according to experimental results presented by Roesler (1979), Stokoe et al. (1985) and Bellotti et al. (1996). Thus, σ'_c could be neglected, and Eq. (4) could be simplified to,

$$V_s = C_s \sqrt{F(e) (\sigma'_a \sigma'_b)^n} \quad [5]$$

In cyclic tri-axial tests, $\sigma'_a = \sigma'_v = \sigma'_1$ and $\sigma'_b = \sigma'_h = \sigma'_3$ based on the installation direction of bender elements as shown in Fig. 6. Therefore, $\sigma'_1 = \sigma'_3 = \sigma'_m$, σ'_m = mean effective stress, for isotropic conditions; $K_0 \sigma'_1 = \sigma'_3$, for anisotropic conditions. Therefore, shear wave velocity achieved by Eq. (5) for isotropic and anisotropic conditions can be determined respectively, by

$$V_s = C_s \sqrt{F(e) \sigma'^{2n}_m} \quad [6]$$

$$V_s = C_s \sqrt{F(e) K_0^n \sigma'^{2n}_1} \quad [7]$$

Substituting $\sigma'_1 = P_a$ into Eq. (2) and Eq. (7)

$$V_{s1} = V_s = C_s \sqrt{F(e) K_0^n P_a^{2n}} \quad [8]$$

Solving C_s by Eq. (6) and substituting it into Eq. (8)

$$V_{s1} = V_s K_0^{0.5n} \left(\frac{P_a}{\sigma'_m} \right)^n \quad [9]$$

Therefore, the stress-corrected shear wave velocity is calculated from the velocities measured in cyclic tri-axial tests using Eq. (9) by assuming n = 0.25 for typical saturated soils. K0 was assumed to be around 0.5 based on the in-situ data from historical liquefied sites (Andrus and Stokoe, 2000; Zhou and Chen, 2007). The confining pressure of 100 kPa was adopted as effective mean stress σ'm for the stress states after normal consolidation and liquefied-reconsolidated process in this study. For the cases of pre-shearing with undraining process, confining pressure was modified by the produced excess pore water pressure using Eq. (9).

4.3.2 Conversion of liquefaction resistance between laboratory and field data

Field-based liquefaction resistances were based on the observation of the occurrences at the ground such as ground settlement, sand boils, footing inclinations during or just after earthquakes. A strain of around 5% with double amplitude produced in the specimen was considered as the criterion to evaluate the liquefaction resistance in cyclic tri-axial tests. The correlated criterion between the two kinds of results was discussed by comparing the data from laboratory and field (Seed et al., 1983; Tokimatsu and Uchida, 1990; Idriss, 1999). Seed et al. suggested the liquefaction resistance be based on the representative number of cycles of different earthquake magnitudes, as shown in Table 2. The equivalent Nc = 15 was adopted in this study for comparing with the field-based data at Mw = 7.5.

The obtained cyclic resistance from tri-axial tests also need to be the converted to field results. Seed (1979) and Kramer (1996) proposed the following equation

$$CRR = 0.9 * C_r * CRR_{tx} \quad [10]$$

Where CRR = cyclic resistance ratio in field; CRRtx= cyclic resistance ratio in tri-axial tests, indicated by the cyclic stress ratio CSR at Nc = 15; Cr = conversion factor, proposed as 0.63 for normal consolidated sandy soil by Seed. Therefore, the laboratory-based data could be evaluated using field-based correlation. The results are shown in Fig. 16.

The laboratory data obtained from tests on Toyoura sand in Fig. 16 represent the possible range in liquefaction resistance that could be expected for sandy soil in the field. The boundary curve of fines contents ≤ 5% was selected for Toyoura sand which is considered without fines. Stress-corrected shear wave velocity could

predict liquefaction resistance of soil experienced by only normal consolidated process (non-pre-shearing) and liquefied-reconsolidated process respectively. The faster stress-corrected velocity indicated the greater liquefaction resistance in sand. Part of the correlation curves both including the two processes entered non-liquefaction territory, that is relative slower velocities indicated smaller liquefaction resistance than the lower bound developed by field-based data. However, the correlation curves did not overlap with each other. The correlation implied that greater liquefaction resistance was achieved by the sand that experienced liquefied-reconsolidated process above the boundary and by the sand without pre-shearing below the boundary when a same stress-corrected velocity was measured. For the cases of pre-shearing with undraining process, the correlation distributed at liquefaction territory and very close to the lower bound.

5. Conclusion

This study discussed the effects of pre-shearing on liquefaction evaluation using shear wave velocity. Cyclic tri-axial tests with bender elements was adopted to investigate the correlation. The factors of different pre-shearing conditions and different relative densities were primarily discussed. The comparison between laboratory-based data for Toyoura sand expected for sandy soils in field and the lower bound for fines content ≤ 5% was conducted. The results verified the applicability of shear wave velocity in assessing liquefaction resistance for pre-sheared sandy soil, and may be more fully described as follows:

For the cases experiencing pre-shearing under undraining process:

1. Shear wave velocity as index can indicate the reduction of liquefaction resistance suffered by pre-shearing.
2. The correlation was influenced by the relative density. Shear wave velocity displayed a similar value under same confining pressure, however, the denser sand achieved greater liquefaction resistance.: Although same confining pressure of 100 kPa was applied during consolidation process, the resistance in denser sand was greater than in looser sand at each shear wave velocities with similar value respectively as shown in Fig. 12.
3. CSR also could be considered as an important factor on the liquefaction resistance at the given shear wave velocity between different relative densities. Liquefaction resistance at same shear wave velocity would be reversed probably at a certain CSR (defined as turning point), and the denser sand achieved the greater resistance if the applied CSR was above the turning point, otherwise, same was probably achieved by the looser sand.

For the cases experiencing the liquefied-reconsolidated process:

1. Shear wave velocity decreased some degree after this process and the difference became larger in the sand with lower B-value.
2. Relative density increased about 5.0% ~6.5% while shear wave velocity decreased about 0 ~16 m/s.
3. Liquefaction resistance would decrease by the effect of this process, especially for the sand with a weak liquefaction resistance initially.

Acknowledgments

The writers are thankful to Mr. Nakashima, Mr. Qin, and Mr. Okri of Kyushu University for their support in conducting the laboratory tests. Liu san, sorry for my late reply. The contribution of Mr. Gobin of Kyushu University is also appreciated for helping the writers proofread the paper. Finally, the writers would like to thank all the anonymous reviewers for their positive criticisms and suggestions.

References

Andrus, R. D., and Stokoe II, K. H., 2000. Liquefaction resistance of soils from shear wave velocity. Journal of Geotechnical and Geoenvironmental Engineering., ASCE, **126** (11), 1015–1025

Arulnathan, R., Boulanger, R. W., and Riemer, M. F., 1998. Analysis of bender element tests. Geotechnical Testing Journal., **21**(2), 120-131.

Bellotti, R., Jamiolkowski, M., Lo Presti, D. C. F., and O'Nell, D. A., 1996. Anisotropy of small strain stiffness in Ticino sand. Geotechnique., **46**(1), 115-131.

Dobry, R., Stokoe II, K. H., Ladd, R. S., and Youd, T. L., 1981. Liquefaction susceptibility from S-wave velocity. Proc., Nat. Convention, In situ Tests to Evaluate Liquefaction Susceptibility, St. Louis, Mo., preprint 81-544,15p.

Hardin, B. O., and Drnevich, V. P., 1972. Shear modulus and damping in soils: design equations and curves. Journal of Soil Mechanics & Foundations Div, ASCE, **98**(SM7), 667-692.

Idriss, I. M., 1999. An update to the Seed-Idriss simplified procedure for evaluating liquefaction potential. Proc., TRB Worshop on New Approaches to liquefaction, FHWA-RD-99-165, Federal Highway Administration,

U.S.A.

Ishihara, K., Tatsuoka, F., and Yasuda, S., 1975. Undrained deformation and liquefaction of sand under cyclic stresses. Soils and Foundations, JGS, **15**(1), 29-44.

Ishihara, K., and Okada, S., 1978. Effects of stress history on cyclic behavior of sand. Soils and Foundations, JGS, **18**(4), 31-45.

Japan Meteorological Agency (2016). The 2016 Kumamoto Earthquake. http://www.data.jma.go.jp/svd/eqev/data/2016_04_14_kumamoto/index.html (In Japanese)

JGS 0544: 2011. Method for laboratory measurement of shear wave velocity of soils by bender element test

Kramer, S. L., 1996. Geotechnical Earthquake Engineering, Prentice Hall, Upper Saddle River, New Jersey 07458, 369-375.

Lade, P. V., and Hernandez, S. B., 1977. Membrane penetration effects in undrained tests. Journal of the Geotechnical Engineering Division, ASCE, **103**(GT8), 914-917.

Lee, J. S., and Santamarina, C., 2005. Bender elements: Performance and signal interpretation. Journal of Geotechnical and Geoenvironmental Engineering, **131**(9), 1063-1070.

Mukunoki, T., Kasama, S., Murakami, H., Ikemi, H., Ishikura, R., Fujikawa, T., Yasufuku, N., and Kitazono, Y., 2016. Reconnaissance report on geotechnical damage caused by an earthquake with JMA seismic intensity 7 twice in 28 h, Kumamoto, Japan. Soils and Foundations, JGS, **56**(6), 947-964.

Robertson, P. K., Woeller, D. J., and Finn, W. D. L., 1992. Seismic cone penetration test for evaluating liquefaction potential under cyclic loading. Canadian Geotechnical Journal, **29**(4), 686-695.

Roesler, S. K., 1979. Anisotropic shear modulus due to stress anisotropy. Journal of the Geotechnical Engineering Division, **150**(7), 871-880.

Seed, H. B., 1979. Soil liquefaction and cyclic mobility evalution for level ground during earthquakes. Journal of Geotechnical and Geoenvironmental Engineering, **105**(GT2), 201-225.

Seed H. B., Idriss, I. M., 1983. Evaluation of liquefaction potential using field performance data. Journal of Geotechnical Engineering, ASCE, **109**(3), 458-482.

Stokoe II, K. H., Lee, S. H. H., and Knox, D.P., 1985. Shear moduli measurements under true triaxial stresses. Advances in the Art of Testing Soils Under Cyclic Conditions. Detroit, ASCE.

Tatsuoka, F., and Ishihara, K., 1974. Yielding of sand in triaxial compression. Soils and Foundations, JGS, **14**(2), 63-76.

Tokimatsu, K., and Uchida, A., 1990. Correlation between liquefaction resistance and shear wave velocity. Soils and Foundations, JGS, **30**(2), 33-42.

Tokimatsu, K., Yamazaki, T., and Yoshimi, Y., 1986. Soil liquefaction evaluations by elastic shear moduli. Soils and Foundations, JGS, **26**(1), 25-35.

Yamada, S., Takamori, T., and Sato, K. 2010. Effects on reliquefaction resistance produced by changes in anisotropy during liquefaction. Soils and Foundations, JGS, **50**(1), 9-25.

Zhou, Y. G., and Chen, Y. M., 2007. Laboratory investigation on assessing liquefaction resistance of sandy soils by shear wave velocity. Journal of Geotechnical and Geoenvironmental Engineering, ASCE, **133**(8), 959-972.

Notation

The following symbols are used in this paper:

CRR	Cyclic resistance ratio
CRR_{tx}	Cyclic resistance ratio in tri-axial tests
CSR	Cyclic stress ratio
C_s	Constant determined empirically
C_r	Conversion factor
C_v	Conversion factor to correct V_s for overburden pressure
DA.	Axial strain with double amplitudes
D_r	Relative density
e_{max}	Maximum void ratio
e_{min}	Minimum void ratio
$F(e)$	Void ratio function
G_s	Specific gravity
K_0	Lateral earth pressure coefficient at rest
L	Length by Top-to-Top between bender elements
Nc	Number of load cycles
P_a	Reference stress
S_r	Saturation degree
V_s	Shear wave velocity
V_{s1}	Stress-corrected shear wave velocity
u	Excess pore water pressure
ΔT	Travel time
σ_1', σ_3'	Major and minor principle effective stresses, respectively
σ_a', σ_b', σ_c'	Principal effective stress acts along the propagation direction, in the direction of particle motion, on the plane, respectively
σ_{c0}'	Effective confining pressure
σ_d	Deviator stress
σ_h'	Effective horizontal effective stress
σ_m'	Mean effective stress
σ_v'	Effective overburden stress